CHEMISTRY
A EUROPEAN JOURNAL

DOI: 10.1002/chem.200902465

Reversible Switching of a Micelle-to-Vesicle Transition by Compressed CO_2

Wei Li,[a] Jianling Zhang,[a] Yueju Zhao,[a] Minqiang Hou,[a] Buxing Han,*[a] Cailan Yu,[b] and Jianping Ye[b]

Abstract: The study of the micelle-to-vesicle transition (MVT) is of great importance from both theoretical and practical points of view. Herein, we studied the effect of compressed CO_2 on the aggregation behavior of dodecyltrimethylammonium bromide (DTAB)/sodium dodecyl sulfate (SDS) mixed surfactants in aqueous solution by means of direct observation, turbidity and conductivity measurements, steady-state fluorescence, time-resolved fluorescence quenching (TRFQ), fluorescence quantum yield, and template methods. Interestingly, all these approaches showed that compressed CO_2 could induce the MVT in the surfactant system, and the vesicles returned to the micelles simply by depressurization; that is, CO_2 can be used to switch the MVT reversibly by controlling pressure. Some other gases, such as methane, ethylene, and ethane, could also induce the MVT of the surfactant solution. A possible mechanism is proposed on the basis of the packing-parameter theory and thermodynamic principles. It is shown that the mechanism of the MVT induced by a nonpolar gas is different from the MVT induced by polar and electrolyte additives.

Keywords: carbon dioxide · micelles · surfactants · transition phases · vesicles

Introduction

The study of mixed surfactant systems is an important topic because the surfactants in the solutions often produce a synergetic effect, new functions, and new organized molecular assemblies. These self-assemblies have been widely used in catalysis, biochemistry, materials synthesis, the petroleum and pharmaceutical industries, and so forth.[1] Mixtures of anionic and cationic surfactants in water often display a range of microstructures, such as spherical micelles, rodlike micelles, vesicles, lamellar phases, and precipitates,[2] due to the electrostatic interactions between the oppositely charged head groups.[3] Study of the transformation from micelles to vesicles is very interesting because such a phenomenon offers, in principle, an easy way of encapsulating active agents by dissolving them in the micellar phase prior to vesicle formation, which is very important from both practical[4] and fundamental[5] points of view. The study of the micelle-to-vesicle transition (MVT) is also of particular relevance for biological systems in which the extraction of proteins from cell membranes is required.[6]

The MVT has been accomplished by changing the anionic/cationic surfactant ratio[4a,7] and temperature[8] and by adding polar additives[9] and salts.[10] It is known that the addition of these additives to surfactant solutions usually suffers from economic and environmental costs and make post-treatment difficult in applications,[11] especially when the system is heat sensitive. More importantly, although organic additives or salts can be used as additives to accomplish the MVT, it is very difficult for them to switch the MVT reversibly.

Supercritical or compressed CO_2 has received much attention over recent years because it is readily available, cheap, nontoxic, and nonflammable. Compressed CO_2 has been used in different fields, such as extraction and fractionation,[12] chemical reactions,[13] materials science,[14] microelectronics,[15] and for the control over the stability of micelles[16] that inhibit the precipitation of surfactants in vesicular systems,[17] the induction of nanoemulsions,[18] the transition between liquid crystals and micelles,[19] the creation of micro-

[a] W. Li, Dr. J. Zhang, Y. Zhao, Dr. M. Hou, Prof. Dr. B. Han
CAS Key Laboratory of Colloid, Interface and Chemical Thermodynamics
Beijing National Laboratory for Molecular Sciences
Institute of Chemistry, Chinese Academy of Sciences
Beijing 100190 (China)
Fax: (+86) 10-62559373
E-mail: hanbx@iccas.ac.cn

[b] C. Yu, J. Ye
CAS Key Laboratory of Photochemistry
Beijing National Laboratory for Molecular Sciences
Institute of Chemistry, Chinese Academy of Sciences
Beijing 100190 (China)

Supporting information for this article is available on the WWW under http://dx.doi.org/10.1002/chem.200902465.

emulsions with CO_2 as the continuous phase,[19,20] and tuning the properties of organic solvents for different processes.[21]

The development of convenient, green, and reversible methods to realize the MVT in surfactant systems is very interesting but challenging. Herein, we found that compressed CO_2 could induce the MVT in a dodecyltrimethylammonium bromide (DTAB)/sodium dodecyl sulfate (SDS) aqueous solution and that the formed vesicles in the solution returned to micelles when the gas was released. In other words, the compressed CO_2 can switch the MVT reversibly only by tuning the pressure of CO_2. As far as we known, this is the first study to carry out and switch a MVT by using a compressed gas. A possible mechanism for this interesting phenomenon, which is different from that of the MVT induced by other additives, such as electrolytes and cosurfactants, is discussed.

Results and Discussion

Phase behavior with and without compressed gas: The DTAB/SDS aqueous solution (20:80, 2 wt%) was transparent and colorless at 25.0°C (Figure 1A, a). The mixed micelle aggregates were formed with an aggregation number of about 210 under these conditions.[22] When compressed CO_2 was charged into the view cell to a certain pressure and stirred for 30 min, the solution exhibited a transition from colorless to slightly bluish (Figure 1A, b–d), which is typical of the presence of vesicles.[8,23] When compressed CO_2 in the cell was released slowly, the solution returned to colorless again (Figure 1A, e), thus showing that the transition was reversible. This outcome is understandable because the gas is very volatile, the dissolved gas was released completely after depressurization,[21] and micellar systems are thermodynamically stable. Therefore, the system returned to the original state.

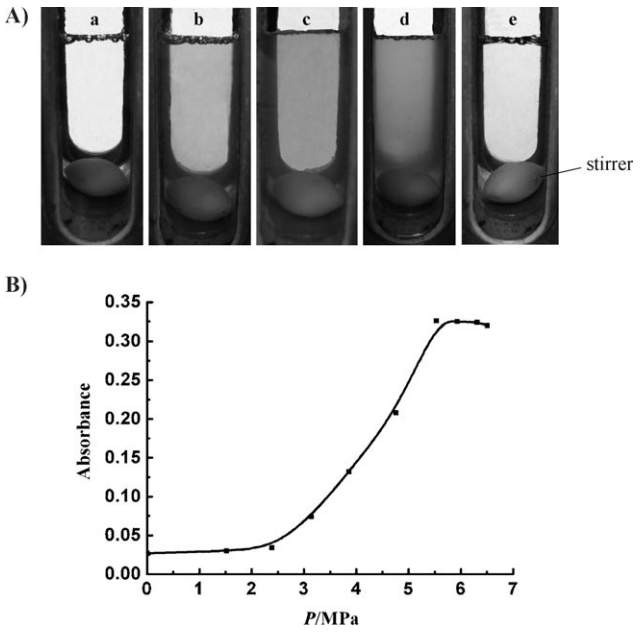

Figure 1. A) Photographs of turbidity variation in the mixed DTAB/SDS aqueous solution (20:80, 2 wt%) at 25.0°C without CO_2 (a); with CO_2 of 3.29 (b), 4.05 (c), 5.50 MPa (d); and after CO_2 was released (e). B) Variation in UV absorbance in the mixed DTAB/SDS aqueous solution (20:80, 2 wt%) at 25.0°C with CO_2 pressure.

UV/Vis spectroscopic analysis is often used to measure the turbidity of solutions.[24] In this study, we studied the turbidity of the surfactant solutions with and without CO_2 by this method (Figure 1B). In the absence of CO_2, UV absorbance of the solution was small and nearly constant as the pressure was less 2.40 MPa, whereas the turbidity increased dramatically as CO_2 pressure exceeded about 2.40 MPa. Herein, we define the pressure at which turbidity begins to increase sharply as the transition pressure P_T because the MVT starts at this pressure, which will be discussed in detail in the following sections. The P_T value of the CO_2/surfactant solution system was about 2.40 MPa (Figure 1B). Figure 1B also indicates that the turbidity of the solution was unchanged with increasing pressure when the pressure was greater than 5.50 MPa. As pressure reached 6.40 MPa, compressed CO_2 liquefied at the experimental temperature, and the experiment was not conducted at higher pressures.

Time-resolved fluorescence quenching (TRFQ): TRFQ is an effective method to measure the transformation of aggregates in surfactant solutions, which has been widely used.[8,25] At the same time, this method is well established for studying the MVT.[8,23,25,26] This technique was used to study the MVT of the solution further. The time-dependent fluorescence intensity of a probe in micelles in the presence of a quencher is thought to obey the Infelta–Tachiya equation (1),[27]

$$I(t) = I(0)\exp\{-A_2t - A_3[1-\exp(-A_4t)]\} \quad (1)$$

where $I(0)$ is the intensity of fluorescence at $t=0$, A_2 is the fluorescence decay rate constant of the probe without a quencher, and A_4 is the quenching rate constant of the probe by a quencher in the micelles. A_2 and A_4 are independent of the concentration of the quencher. A_3 represents the average number of quenchers per micelle and is defined by Equation (2) .[27]

$$A_3 = N[Q]/C_m \quad (2)$$

where N and C_m are the aggregation number and concentration of the surfactant, respectively, and $[Q]$ is the concentration of the quencher. It can be known from Equation (1) that the fluorescence decay curves of the micelle solutions appear to be of a double-exponential form. In vesicles and other large aggregates, the time-dependent fluorescence intensity of a probe in the presence of a quencher is thought to obey the modified Stern–Volmer equation [Eq. (3)]:[28]

$$I(t) = I(0)\exp\{-A_5t - A_6t^{1/2}\} \quad (3)$$

Both A_5 and A_6 depend on the concentration of the

quencher. Thus, the decay curves of samples containing large aggregates appear in a monoexponential form. If micelles and vesicles coexist in the solution, the fluorescence decay curves obey a linear combination of Equations (1) and (3). If the curves are forced to fit the form of Equation (1), A_4 shows dependence on the concentration of the quencher and the ratio of vesicles to micelles.[8,26] The experimental data gradually departs from Equation (1) when the ratio of vesicles to micelles increases. At a very high ratio of vesicles to micelles, the data do not obey Equation (1) and Equation (3) should be used. Hence, TRFQ can be used to track the transition between the micelles and vesicles and is employed to verify the MVT induced by compressed CO_2 herein.

The TRFQ data for the DTAB/SDS system under different pressures of CO_2 were measured. The variation of A_4 [obtained by fitting the data to Equation (1)] as a function of η ($\eta=[Q]/C_m$; C_m is the total concentration of the surfactants) for these solutions is shown in Figure 2. Before the

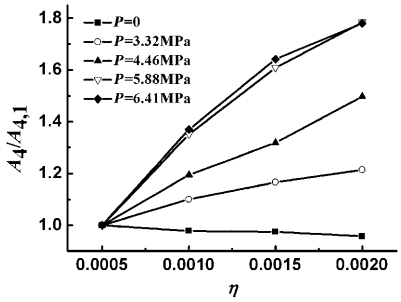

Figure 2. Normalized value of the parameter A_4 in Equation (1) as a function of η ($\eta=[Q]/C_m$) at 25.0 °C and different CO_2 pressures for the DTAB/SDS aqueous solution (20:80, 2 wt %).

addition of CO_2, A_4 was almost independent of η, that is, all the surfactant aggregates in the solution were micelles, as was previously reported.[8,26] After the addition of CO_2, the slope of A_4 versus η began to deviate from zero, thus indicating that the formation of vesicles is gradual. With an increase in the pressure of CO_2, the slope of $A_4/A_{4,1}$ ($A_{4,1}$ is the value of A_4 at $\eta=0.0005$) versus η increased, thus suggesting that the ratio of vesicles to micelles increased, as proved by others.[8,25,26] Figure 2 also demonstrates that the plots of A_4 versus η at 5.88 and 6.41 MPa were nearly same. This finding indicates that the ratio of vesicles to micelles did not change with pressure as the pressure was high enough, which is consistent with the conclusion obtained from the turbidity study (Figure 1B).

Conductivity study: Conductivity determination is one of the most useful techniques to study aggregation in surfactant solutions,[29] and the results can provide information on the transition from micelles to vesicles.[30] This method was used in this study. We can see from Figure 3 that the conductivity increased with increasing pressure of CO_2 when the pressure was less than approximately 2.40 MPa, decreased quickly

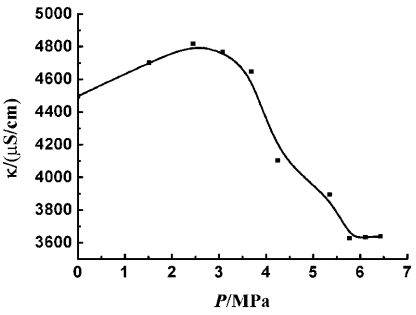

Figure 3. Dependence of conductivity of the DTAB/SDS aqueous solution (20:80, 2 wt %) on CO_2 pressure at 25.0 °C.

with increasing pressure at 2.40–5.70 MPa, and then increased slightly again with a further increase in pressure. The conductivity originated mainly from the surfactant ions and the ionization of CO_2. Therefore, the addition of CO_2 affects conductivity mainly in two opposite ways. On one hand, CO_2 in water can be partially ionized (i.e., $H_2O+CO_2\rightarrow H^+ + HCO_3^-$), which should increase the conductivity and the effect should be larger at higher pressure.[31] On the other hand, CO_2 can induce the MVT when the pressure is high enough (see above). The surfactant molecules in the vesicle bilayer do not contribute to the conductivity any further after the bilayer segments close up to form vesicles, which results in a decrease in conductivity.[30a] As the pressure of CO_2 was lower than approximately 2.40 MPa, the formation of vesicles was not significant. Therefore, the first factor was dominant, and the conductivity increased with increasing pressure. On further increasing the pressure, the conductivity curve showed a significant decrease with increasing pressure up to 5.50 MPa because more vesicles were formed. This behavior was similar to the conductivity of the MVT process induced by other methods.[31,32] Therefore, it can be concluded that the second factor became dominant in this pressure region. When the pressure was greater than approximately 5.50 MPa, the conductivity increased slightly with increasing pressure because the MVT had finished. Therefore, the conductivity results further support the argument that MVT occurred in the pressure region of approximately 2.40–5.50 MPa.

Fluorescence-probe study: The use of fluorescence probes is a sensitive technique for evaluating the physicochemical properties of molecular aggregates.[33] The fluorescence probe Nile red (NR) has been used extensively as a probe for vesicular systems due to its hydrophobic nature, which allows the probed to be incorporated into the bilayer moiety.[34] In addition, this probe exhibits solvatochromic behavior and a redshift in the emission maximum can be observed in polar media, together with fluorescence quenching, due to the capability of NR to form hydrogen bonds with protic solvents.[35] Therefore, this approach was very useful in studying the MVT.[36] To further confirm the occurrence of MVT in solution, NR was used as a probe to investigate the MVT induced by CO_2. Figure 4 gives the emission

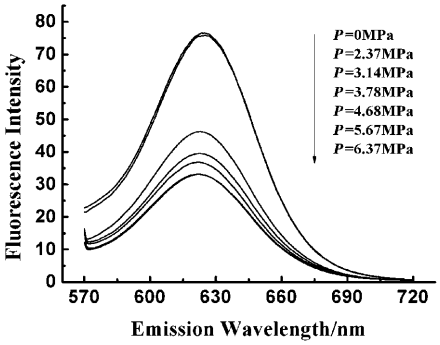

Figure 4. Fluorescence spectra of Nile red in DTAB/SDS aqueous solution (20:80, 2 wt%) at some typical CO_2 pressures ($\lambda_{ex}=550$ nm).

spectra of NR in the SDS/DTAB/water system at 25.0°C and different pressures. A decrease in intensity was not detectable when the pressure of CO_2 was below 2.40 MPa. After this point, the emission intensity decreased rapidly with increasing pressure, thus indicating that NR was present in a more hydrophobic environment. It is known that the bilayer region of vesicles is usually more hydrophobic than the interfacial region of micelles.[34a,b,37] Therefore, the decrease in the intensity of the NR fluorescence justified the argument that the amount of vesicles increased with increasing pressure of CO_2. The phenomenon was consistent with previous reports of the MVT.[37] When the pressure was over 5.50 MPa, the emission intensity was unchanged with increasing pressure, thus implying that the MVT had finished. The same trend was also observed in the variation of the maximum emission wavelength λ_{max} of NR (Figure 5). There

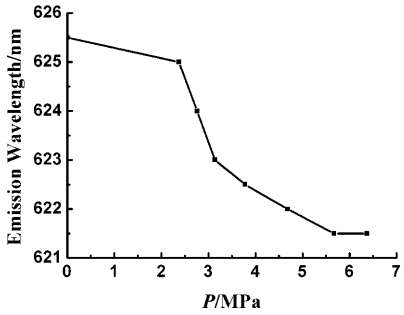

Figure 5. Dependence of maximum emission wavelength of Nile red in DTAB/SDS aqueous solution (20:80, 2 wt%) on CO_2 pressure at 25.0°C.

was a little change in the λ_{max} value when the pressure was below 2.40 MPa. On further increasing the pressure of CO_2, the λ_{max} value decreased considerably from $\lambda_{max}=625.5$ to 621.5 nm, thus indicating that NR was present in a more hydrophobic environment at higher pressures. This result was similar to the reported transformation process of micelles to vesicles.[38] When the pressure was over 5.50 MPa, the maximum emission wavelength was nearly constant on increasing the pressure. This outcome shows that the structure of the aggregates did not change when the pressure was over 5.50 MPa. The change in the fluorescence spectra of NR and the λ_{max} value gives clear information about the MVT with the addition of compressed CO_2, which is consistent with the TRFQ and conductivity studies discussed above.

The fine structure of pyrene fluorescence presented five peaks. The ratio between the intensities of the first and third peaks in the spectrum ($\lambda=372$ and 382 nm and denoted as I_1 and I_3, respectively) is related to the polarity of the pyrene microenvironment.[39] A low value for the ratio corresponds to a nonpolar environment. The ratio decreases as the polarity of the microenvironment is decreased. This method is often used to monitor the course of the MVT in the cationic/anionic surfactant systems.[37,40] In the micelle solution, pyrene may easily enter the inner nonpolar center of the micelles and show the local environment. In vesicles, pyrene is solubilized in the bilayer.[41] It has been demonstrated that the I_1/I_3 ratio decreases when micelles transform into vesicles in the mixed surfactant solutions.[37] Figure 6

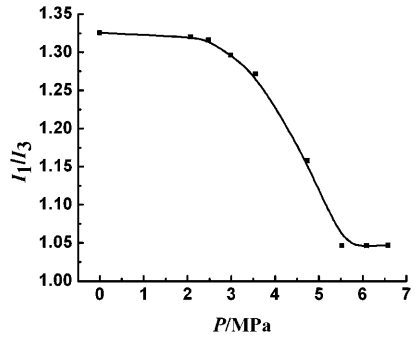

Figure 6. Dependence of I_1/I_3 of pyrene in DTAB/SDS aqueous solution (20:80, 2 wt%) on CO_2 pressure at 25.0°C.

shows the I_1/I_3 ratios at different pressures of CO_2 in the surfactant system studied. At lower pressure, the curve was flat, thus indicating that the transformation was not significant in the solution. In the pressure range of approximately 2.40–5.50 MPa, the ratio decreased from 1.33:1 to 1.04:1. Therefore, the decrease in the I_1/I_3 ratio over this pressure supported the argument that the micelles transformed into vesicles gradually in solution with increasing pressure of CO_2. When the pressure reached 5.50 MPa, the ratio did not change on further increasing the pressure (Figure 6), thus indicating that all the micelles were transformed into vesicles. This conclusion is the same as that obtained by the previously discussed methods.

Auramine is another useful fluorescence probe to study the structure of surfactant solutions. It has been reported that the fluorescence intensity of auramine solubilized in a surfactant solution increases due to the prevention of intermolecular motion as a result of the increasing viscosity around the solubilized position.[42] Therefore, the fluorescence intensities of auramine with and without the surfactant (I and I_0, respectively) in a I/I_0 ratio were employed as an indicator to study the microviscosity of the aggregates in surfactant solutions.[30] We used auramine as the probe to investigate the MVT in the surfactant solution. Figure 7 illus-

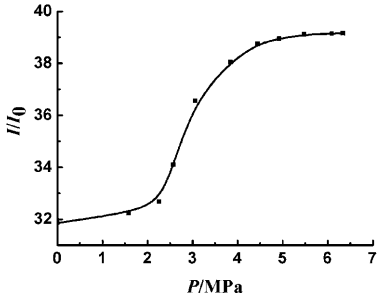

Figure 7. Dependence of I/I_0 of auramine in DTAB/SDS aqueous solution (20:80, 2 wt %) on CO_2 pressure at 25.0 °C.

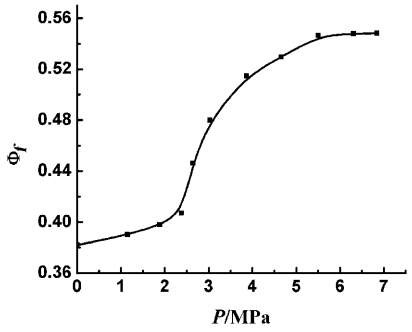

Figure 8. Dependence of fluorescence quantum yield Φ_f of DPB in DTAB/SDS aqueous solution (20:80, 2 wt %) on CO_2 pressure at 25.0 °C.

trates the I/I_0 ratio of auramine in the DTAB/SDS solution at different pressures of CO_2. At lower pressures, the I/I_0 ratio changed slowly with pressure, thus indicating that a little transition occurred in the solution. A slight increase in I/I_0 ratio indicates an increase in microviscosity, for which the main reason may be that CO_2 can expand the micelles.[43] The I/I_0 ratio increased sharply after the pressure increased to more than approximately 2.40 MPa. It is known that the microviscosity of vesicles is larger than that of micelles.[40] A significant change in I/I_0 ratio also suggests a MVT, and this phenomenon is consistent with the MVT accomplished by other methods.[30a,36a,40] Similarly, the I/I_0 ratio did not change after approximately 5.50 MPa, thus suggesting that all the micelles completely transformed into vesicles. Therefore, the results also suggest that the MVT occurred mainly in the pressure range 2.40–5.50 MPa.

Fluorescence quantum yield measurements: Fluorescence quantum yield measurements were also employed to obtain information about MVT in the surfactant solutions.[44] The rigidity of the microenvironment can impact on the observed fluorescence quantum yields by restricting certain vibrational modes within the excited-state fluorophore, which may lead to the ground state through nonradiative decay processes.[45] A typical curve of the fluorescence quantum yield Φ_f of *trans*,*trans*-1,4-diphenyl-1,3-butadiene (DPB) in DTAB/SDS solution at different pressures of CO_2 determined herein is shown in Figure 8. Similarly, the quantum yield increased slowly with pressure below approximately 2.40 MP, and increased quickly when the pressure was further increased because of rupture of the micelles and formation of vesicle membranes. Furthermore, the probes "felt" the presence of a more ordered phase because of the formation of vesicles.[44a,45] Over 5.50 MPa, the Φ_f value was constant, thus demonstrating that there was no obvious change in the aggregate structure in the solution.[44]

Preparation of silica particles by using the surfactant aggregates as a template: Micelles and vesicles are commonly used templates to synthesize various kinds of materials.[46] It is well known that water becomes acidic after dissolving CO_2 and returns to neutral after releasing CO_2. At the same time, tetraethoxysilane (TEOS) can hydrolyze to form silica under acidic conditions.[47] To obtain more information about the MVT, the surfactant solution with and without CO_2 was used as a template to prepare silica particles. CO_2 acted both as the catalyst and reagent to control the morphology of the template. The TEM images of the silica particles obtained are shown in Figure 9. Only silica spheres of less than 50 nm were formed in the absence of CO_2 (Figure 9 a), which is a typical size of micelles and indicates that only micelles existed in the system without CO_2. This finding

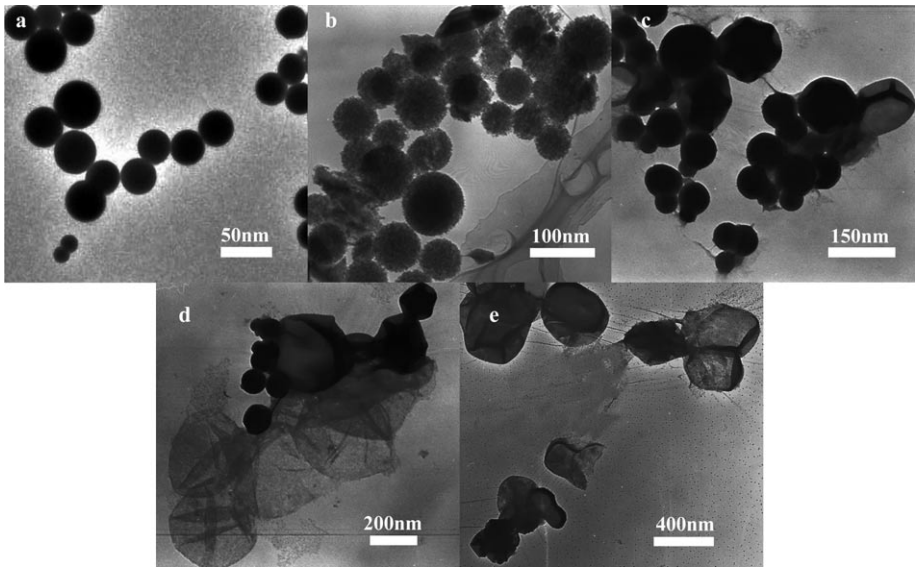

Figure 9. TEM images of silica particles prepared in DTAB/SDS aqueous solution; a) without CO_2 and with CO_2 by using sulfuric acid as the catalyst at pH 3.0, and with CO_2 at pressures of b) 1.96, c) 2.57, d) 5.06, and e) 6.02 MPa.

agrees with a previously reported conclusion.[22] Larger spheres were obtained at 1.96 MPa (Figure 9b), thus indicting that CO_2 can swell the micelles, similar to the way that CO_2 swells liquid-crystal films.[43] Silica particles formed with micelles as the template and some vesicle-like silica particles were formed at 2.57 MPa (Figure 9c), thus indicating that the MVT occurred because the morphology of the silica particles directly reflected that of the templates. The size of the vesicle-like silica particles increased with increasing the pressure of CO_2 (Figure 9c,d). However, the silica particles with both the micelle and vesicle templates were formed at 2.57 and 5.06 MPa, thus suggesting that both micelles and vesicles existed in the solution at these pressures. Only the vesiclelike silica particles existed in the system at 6.02 MPa (Figure 9e). These results further support the pressure range of the MVT discussed above. On the other hand, this finding provides a method to control the morphology of the silica particles synthesized.

Possible mechanism: As far as we know, this is the first report of a MVT induced by a compressed gas. To obtain more information about the mechanism of the MVT, we conducted some control experiments.

It is well known that CO_2 can dissolve in water and can be ionized partially (i.e., $H_2O+CO_2 \rightarrow H^+ + HCO_3^-$), which makes the water acidic and the pH value can be lowered to pH 3.20 at 6.00 MPa.[31] To clarify the effect of pH value on the stability of the micelles, we used citric acid buffers to fix the pH values of the DTAB/SDS solution in the absence of CO_2. The pH values of the solution were pH 3.0, 4.0, 5.0, and 6.0, respectively, and it was shown that the pH value did not noticeably affect turbidity. This finding suggested that the change in acidity caused by CO_2 was not the reason for the MVT. We also studied the possibility of inducing the MVT in the SDS/DTAB system by using other gases, including methane, ethylene, and ethane. Similar to CO_2, the gases could also change the solution from colorless to bluish, and the turbidity increased dramatically after certain pressures were reached (Figure 10), which suggests that these gases could also induce the MVT. This outcome further supports the argument that the change in the water caused by CO_2 was not the main reason for the MVT because the solubility of hydrocarbon gases in water is negligible. We also investigated the effect of the pressure of helium on the transformation up to 8.00 MPa, which can be considered to be the effect of pressure only because the solubility of the gas in the liquids is extremely small.[48] The results by direct-observation, UV/Vis spectroscopic, and fluorescence (pyrene as the probe) methods are given in the Supporting Information (Figures S1–S3). It was demonstrated that the turbidity of the solution and the I_1/I_3 ratio did not change with pressure, which ruled out the possibility that the MVT was induced by hydrostatic pressure. This outcome is similar to the conclusion that the effect of pressure itself on the structure of $C_{12}E_6$ micelles in aqueous solution was very limited up to 9.00 MPa,[49] and the influence of hydrostatic pressure on the ordered structure of dipalmitoylphosphatidylcholine was

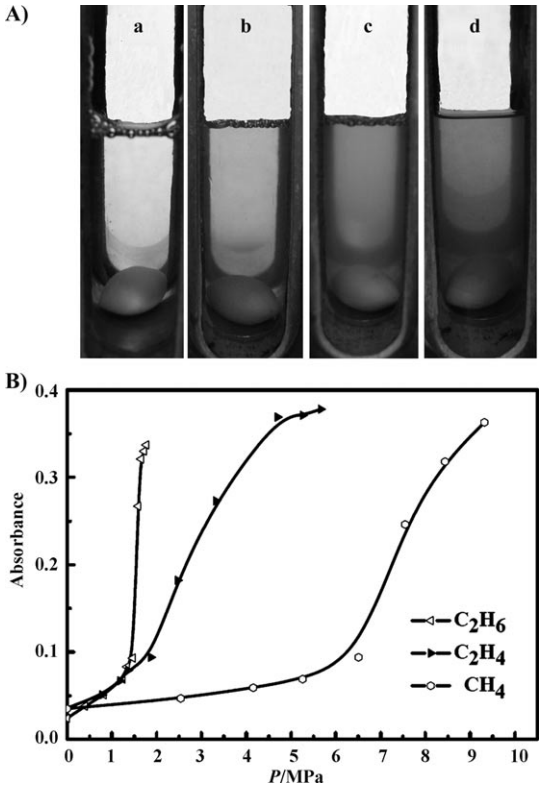

Figure 10. A) Photographs of the DTAB/SDS aqueous solution (20:80, 2 wt%) at 25.0 °C without gas (a) and with methane at 7.50 MPa (b), ethylene at 4.20 MPa (c), and ethane at 1.54 MPa (d). B) Turbidity variation in the DTAB/SDS aqueous solution (20:80, 2 wt%) at 25 °C with methane, ethylene, and ethane at different pressures.

negligible up to 14.00 MPa.[50] We also studied the possibility of inducing the MVT by using three liquid alkanes, including *n*-pentane, *n*-heptane, and *n*-octane. They were added into the DTAB/SDS solution, respectively. It was demonstrated that non of the liquid alkanes could induce the MVT, and phase separation occurred if too much liquids were added. This illustrated that only the hydrocarbon gases of small size could induce the MVT.

Through a combination of the above experimental results and the aggregate packing parameter theory,[51] we propose a possible mechanism for the MVT induced by compressed CO_2 (see Figure 11 for a schematic illustration). The packing parameter is equal to $V_c/(a_0 l_c)$, where V_c and l_c are the chain volume and chain length of the hydrophobic group, respectively, and a_0 is the optimum area per polar group.[51] Obviously, the curvature of the interfacial film decreases with an increasing the value of the packing parameter. A larger packing parameter is favorable for the formation of vesicles due to the smaller curvature of the interfacial films, whereas micelles are formed at a small packing parameter.[51b] This conclusion is also supported by the fact that the size of the silica particles formed from the micelle template could be expanded by CO_2 only up a certain size (Figure 9). As discussed above, the MVT induced by CO_2 does not originate from the change in the water. It has been reported that CO_2 is very soluble in *n*-dodecane[52] and other organic

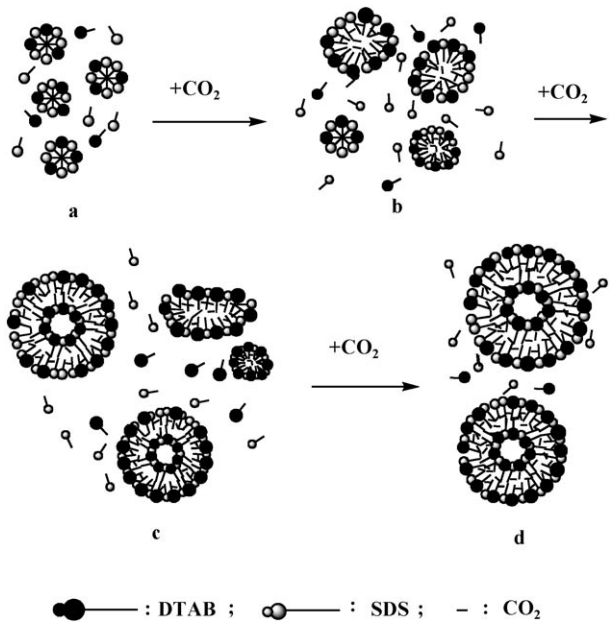

Figure 11. Illustration of the possible mechanism of a MVT with compressed CO_2. a) SDS/DTAB mixed micelles; b) micelles are expanded at the lower pressure; c) micelles/vesicles coexist in the pressure range of approximately 2.40–5.50 MPa; d) only vesicles exist in the system.

solvents.[21] Therefore, we can deduce that CO_2 can insert into the hydrocarbon-chain region of the surfactant films, although it is very difficult to determine the exact solubility of CO_2. The insertion of CO_2 into the hydrocarbon-chain region is similar to increasing volume of the hydrocarbon chains because the gas has a volume, which decreases the curvature of the interfacial films, that is, the packing parameter becomes larger. This deduction is supported by the fact that CO_2 can swell micelles and that the silica particles prepared at 1.96 MPa were larger than the particles fabricated in the absence of CO_2 (Figure 9). More CO_2 is inserted into the hydrocarbon-chain region at higher pressure, and therefore the packing parameter increases with increasing pressure. When the packing parameter is large enough, vesicles begin to form in the solution. On increasing the pressure of CO_2, more micelles transform into vesicles because the micelles are not stable at a large value of the packing parameter. At a certain pressure region, vesicles/micelles coexist, similar to when MVT is induced by salt and temperature.[8,10a] Eventually, vesicles are much more stable in the solution and all the aggregates exist as vesicles. From a thermodynamic point of view, we can consider that a complex equilibrium exists between micelles and vesicles in the system in the presence of CO_2. The addition of CO_2 can shift the equilibrium in the direction of the formation of vesicles, and the vesicles are much more stable thermodynamically than micelles when enough CO_2 is added.

As discussed above, large alkanes could not induce a MVT in the surfactant system. The main reasons may be that it is difficult for the larger molecules to accommodate themselves in the interfacial film stably or the ordered film is not stable if large molecules insert into the chain region. The detailed reasons need to be studied further.

Some polar additives and electrolytes can also induce a MVT under suitable conditions. Generally, it is considered that these additives dehydrate the surfactant head groups and decrease electrostatic repulsions. So the head groups of the surfactants in the interfacial film are packed more closely, which causes a decrease in the a_0 value and consequently an increase in the packing parameter.[53] This mechanism is different from a MVT induced by CO_2. In other words, polar additives and electrolytes induce a MVT by decreasing the a_0 value in the expression $V_c/(a_0 l_c)$, whereas CO_2 induces a MVT by increasing the V_c value.

Conclusions

Herein, we have found that compressed CO_2 can reversibly switch the MVT in a DTAB/SDS system by controlling the pressure under suitable conditions. This detailed study indicates that the MVT induced by CO_2 does not originate from a change in one of the properties of water. The main reason may be that CO_2 can insert into the hydrocarbon-chain region of the interfacial films, which increases the structural packing parameter. Other gases, such as methane, ethylene, and ethane, could also induce the MVT in the mixed surfactant solution. The mechanism of a MVT induced by a gas is different from that of a MVT induced by polar additives and electrolytes. Generally, it is considered that these additives decrease electrostatic repulsions between the polar heads of the surfactants, which causes a decrease in the a_0 value and consequently an increase in the structural-packing parameter, whereas a nonpolar gas increases the V_c value. Switching the MVT by using CO_2 may find different applications in materials science and chemical reactions.

Experimental Section

Materials: Dodecyltrimethylammonium bromide (DTAB; >99% purity) and sodium dodecyl sulfate (SDS; A.R. grade) were purchased from the Shanghai Shanpu Chemical Corporation and Tianjin Jinke Fine Chemical Institute, respectively. These compounds were recrystallized five times from ethanol/acetone before use. 9-(Diethylamino)-5*H*-benzo[α]phenoxazin-5-one (Nile red), 1,6-dipheny-1,3,5-hexatriene, cetylpyridinium chloride (CPC), and pyrene were supplied by Sigma. Auramine and *trans*,-*trans*-1,4-diphenyl-1,3-butadiene (DPB) were provided by Aldrich. Tetraethoxysilane (TEOS) was purchased from the Tianjin Yongda Chemical Reagent Company. Sulfuric acid (A.R. grade) was produced by the Beijing Chemical Factory. Carbon dioxide, methane, ethylene, and ethane (>99.9% purity) were provided by the Beijing Analytical Instrument Factory. *n*-Pentane, *n*-heptane, and *n*-octane were purchased from the Beijing Yili Chemical Reagent Company. Double-distilled water was used throughout the experiments. The molecular structures of the fluorescence probes are given in the Supporting Information.

Phase-behavior investigation: The apparatus and procedures to study the phase behavior of the surfactant systems were the same as those used previously.[54] The apparatus consisted mainly of a view cell (34.0 mL) with a magnetic stirrer, a high-pressure pump (DB-80), a constant-temperature water bath, and a pressure gauge. The accuracy of the pressure

gauge, which was composed of a transducer (FOXBORO/ICT, Model 93) and an indicator, was ±0.025 MPa within the pressure range 0—20 MPa. The temperature of the water bath was controlled by an HAAKE D8 temperature controller with an accuracy of ±0.1 °C.

In the experiment, the surfactant solution was loaded into the view cell, which was placed in a water bath of 25.0 °C. CO_2 was charged into the view cell to a suitable pressure. The magnetic stirrer was used to accelerate the mixing of CO_2 in the surfactant solutions. After the system reached equilibrium, the stirrer was stopped, the phase behavior was observed, and a photo was taken.

Turbidity measurement: UV/Vis spectroscopic analysis was used to study the turbidity of the surfactant systems with and without CO_2. The apparatus and procedures were similar to those reported previously.[55] The apparatus consisted mainly of a gas cylinder, a high-pressure pump, a pressure gauge, a UV/Vis spectrometer, and a temperature-controlled high-pressure UV sample cell. The UV/Vis spectrophotometer was produced by the Beijing General Instrument Company (Model TU-1201) and had a resolution of 0.1 nm. The sample cell was composed mainly of a stainless steel body, two quartz windows, a stirrer, and a temperature-controlling system. The optical path length and the inner volume of the cell were 2.1 cm and 8.8 mL, respectively.

To determine the turbidity, the absorbance at $\lambda = 514.5$ nm was monitored at which no absorbance was observed for the surfactant system.[23] In the experiment, the sample cell was flushed with CO_2 to remove the air in the cell. The surfactant solution was charged into the sample cell of 25.0 °C and the solution was stirred. The UV absorbance was recorded at different times. CO_2 was compressed into the sample cell to the desired pressure. The stirrer was stopped after 1 h, and the UV absorbance of the solution was recorded at different times until the absorbance was independent of time. The procedures for other gases were similar, with the only difference that other gases were used.

Conductivity measurements: The apparatus for the conductivity measurements was similar to that for studying the reverse micellar solutions reported previously.[56] The apparatus consisted mainly of a high-pressure stainless steel vessel, a conductivity cell, a constant temperature water bath, a high-pressure syringe pump, a pressure gauge, a magnetic stirrer, and a gas cylinder. The temperature of the water bath was controlled using an HAAKE D8 controller. A conductivity meter with a precision of ±0.5 %, which was produced by the Shanghai Precision Scientific Instrument Co. (Model DDS-307), was used to determine the conductivity. Both the working and counter electrodes were made of Pt foil (thick: 0.3 mm). The cell constant was calibrated with solutions of aqueous KCl of different concentrations. In a typical experiment, a suitable amount of surfactant solution was charged into the high-pressure stainless-steel vessel. The vessel was placed in a constant-temperature water bath of 25.0 °C. After thermal equilibrium had been reached, CO_2 was charged into the system until a suitable pressure was reached. A magnetic stirrer was used to enhance the dissolution of CO_2 in the solution. After the system stabilized, which was known from the fact that both pressure and conductivity were independent of time, the conductivity of the solution was recorded.

Time-resolved fluorescence quenching (TRFQ): The sample cell was the same as that used in steady-state fluorescence measurements of micellar solutions.[57] The cell was composed mainly of a stainless-steel body with four channels, four-quartz windows (diameter: 1.6 cm, thickness: 0.7 cm). The inner volume of the sample cell was 8.44 mL and was thermostated to ±0.2 °C of the desired temperature with a heater and temperature controller. The experimental procedures were also similar to those reported previously.[57] In the experiments, pyrene was used as the fluorescence probe, and CPC (see Scheme S1 in the Supporting Information) to quench the probe. The desired amounts of pyrene in ethanol and CPC in water were added to the surfactant solution directly, and the solution was stirred vigorously for 48 h. The concentration of pyrene was kept low (1 μM) to prevent excimer formation. All of the solutions were degassed with nitrogen for 15 min before the measurement to eliminate the influence of oxygen. Pyrene fluorescence decay curves were recorded by an Edinburgh FLS920 time-resolved fluorescence spectrophotometer (excitation and emission at $\lambda_{ex} = 337$ and $\lambda_{em} = 385$ nm, respectively). The fluorescence decay of pyrene was fitted by using modified DECAN 1.0 software.

Steady-state fluorescence measurements: The apparatus and procedures used for the steady-state fluorescence spectroscopic measurements were similar to those reported previously.[56,57] The apparatus consisted mainly of a gas cylinder, a high-pressure pump, fluorescence spectrophotometer (F-2500, Hitachi), and a high-pressure fluorescence sample cell. The emission spectra were recorded on the spectrophotometer equipped with a computer. A Xe lamp was used as the excitation resource. No additional filters were used.

Three fluorescence probes, pyrene, Nile red, and auramine (see Scheme S1 in the Supporting Information) were used in the experiments. Solutions of pyrene or Nile red in ethanol were introduced into the surfactant systems, and their final concentrations in the surfactant solution were 5 and 3 μM, respectively, which were similar to that reported by other studies.[22,58] Aqueous solutions of auramine were injected into the surfactant solution, thus giving a concentration of about 10 μM in the surfactant solution. Excitation wavelengths of $\lambda_{ex} = 550$, 380, and 335 nm were chosen for pyrene, auramine, and Nile red, respectively, and the emission wavelengths of these probes were $\lambda_{em} = 350$–500, 430–600, and 570–750 nm, respectively. In all cases, the scan rate was 60 nm min^{-1}. For pyrene, the excitation and emission slit widths were kept at 5.0 and 2.5 nm, respectively. For the other two probes, the slit widths were kept at 5.0 nm.

In the experiments, the air in the sample cell was first replaced by CO_2. The temperature of the cell was maintained at 25.0 °C. A suitable amount of surfactant solution with the probe was loaded into the sample cell, and the fluorescence spectra were recorded after the system reached thermal equilibrium. CO_2 was charged by using a high-pressure pump until the desired pressure was reached. The fluorescence spectra were recorded until the intensity did not change with time.

Fluorescence quantum yield measurements: Equation (4) was used to obtain the fluorescence quantum yield Φ_f of the fluorescence probe DPB (see Scheme S1 in the Supporting Information).[59]

$$\Phi_f = [I\Phi_{f0})/I_{f0}][(1 - 10^{-A_{f0}})/(1 - 10^{-A_{f0}})] \quad (4)$$

where Φ_f, Φ_{fo}, I_f, and I_{fo} are the quantum yields and fluorescence intensities of the probe in the surfactant solution and reference solution, respectively. A_f and A_{fo} are the UV absorbances of the probe in the surfactant solution and reference solution, respectively, measured at $\lambda = 340$ nm. The excitation wavelength was also $\lambda = 340$ nm. In this study, we used DPB/cyclohexane as the reference solution to give $\Phi_{fo} = 0.44$ at 25.0 °C.[59] Further details on the calculation of Φ_f have been reported in previously.[59,60]

Preparation of silica particles by using the surfactant solution as a template: The apparatus was similar to that used in the study of the effect of CO_2 on the phase behavior of the mixed surfactant system (see above). In the experiment, DTAB/SDS solution (20:80, 2 wt %, 10.0 mL) was charged into the view vessel. TEOS (0.2 mL) was added into the system and stirred for 24 h at 25.0 °C. After depressurization, the upper white latex was collected and washed with water and ethanol. Experiments without CO_2 were also conducted, and the procedures were similar to that described above. The main difference was that a small amount of sulfuric acid was used as the catalyst for the hydrolysis reaction of TEOS and the pH value of the solution was 3.0. The morphology of the obtained particles was characterized by using TEM with a TECNAI 20 PHILIPS electron microscope. The particles were dispersed in ethanol and directly deposited on the copper grid.

Acknowledgements

This work was supported by the National Natural Science Foundation of China (20633080, 20873164), the Ministry of Science and Technology of China (2009CB930802), and the Chinese Academy of Sciences (KJCX2.YW.H16).

[1] a) D. Sun, A. E. Riley, A. J. Cadby, E. K. Richman, S. D. Korlann, S. H. Tolbert, *Nature* **2006**, *441*, 1126–1130; b) T. Zemb, M. Dubois, B. Demé, T. Gulik-Krzywicki, *Science* **1999**, *283*, 816–819; c) M. J. Hollamby, K. Trickett, A. Vesperinas, *Chem. Commun.* **2008**, 5628–5630; d) M. Nichifor, M. Bastos, S. Lopes, *J. Phy. Chem. B* **2008**, *112*, 15554–15561.
[2] a) K. L. Herrington, E. W. Kaler, D. D. Miller, J. A. Zasadzinski, S. Chiruvolu, *J. Phys. Chem.* **1993**, *97*, 13792–13802; b) M. Dubois, B. Demé, T. Gulik-Krzywicki, J. C. Dedieu, C. Vautrin, S. Désert, E. Perez, T. Zemb, *Nature* **2001**, *411*, 672–675.
[3] A. J. O'Connor, T. A. Hatton, A. Bose, *Langmuir* **1997**, *13*, 6931–6940.
[4] a) M. J. Russell, *Science* **2003**, *302*, 580–581; b) J. S. Martinez, G. P. Zhang, P. D. Holt, H. T. Jung, C. J. Carrano, M. G. Haygood, A. Butler, *Science* **2000**, *287*, 1245–1247.
[5] a) M. Martin, S. M. Hanczyc, J. W. Szostak, *Science* **2003**, *302*, 618–622; b) S. Laurent, D. Forge, M. Port, A. Roch, C. Robic, L. V. Elst, R. N. Muller, *Chem. Rev.* **2008**, *108*, 2064–2110.
[6] a) B. Matthew, K. Dickerson, H. Sandhage, R. R. Naik, *Chem. Rev.* **2008**, *108*, 4935–4978; b) S. Sonnino, A. Prinetti, L. Mauri, V. Chigorno, G. Tettamanti, *Chem. Rev.* **2006**, *106*, 2111–2125.
[7] A. E. Speers, C. C. Wu, *Chem. Rev.* **2007**, *107*, 3687–3714.
[8] H. Q. Yin, S. Lei, S. Zhu, J. B. Huang, J. P. Ye, *Chem. Eur. J.* **2006**, *12*, 2825–2830.
[9] V. N. Filipovič, M. Bujan, I. Sÿmit, L. Tušek, I. Sÿtefanič, *J. Colloid Interface Sci.* **1998**, *201*, 59–64.
[10] a) S. H. Tung, H. Y. Lee, S. R. Raghavan, *J. Am. Chem. Soc.* **2008**, *130*, 8813–8817; b) L. Hao, Y. Nan, H. Liu, Y. Hu, *J. Dispersion Sci. Technol.* **2006**, *27*, 271–273.
[11] Y. Liu, P. G. Jessop, M. Cunningham, C. A. Eckert, C. L. Liotta, *Science* **2006**, *313*, 958–961.
[12] a) L. A. Blanchard, D. Hancu, E. J. Bechman, J. F. Brennecke, *Nature* **1999**, *399*, 28–29; b) E. Reverchon, I. De Marco, *J. Supercrit. Fluids* **2006**, *38*, 146–166.
[13] a) D. J. Cole-Hamilton, *Science* **2003**, *299*, 1702–1706; b) P. G. Jessop, *J. Supercrit. Fluids* **2006**, *38*, 211–231; c) T. Oku, Y. Arita, H. Tsuneki, T. Ikariya, *J. Am. Chem. Soc.* **2004**, *126*, 7368–7377.
[14] a) K. P. Johnston, P. S. Shah, *Science* **2004**, *303*, 482–483; b) A. I. Cooper, *Adv. Mater.* **2001**, *13*, 1111–1114.
[15] a) J. Keagy, X. G. Zhang, K. P. Johnston, E. Busch, F. Weber, P. J. Wolf, T. Rhoad, *J. Supercrit. Fluids* **2006**, *39*, 277–285; b) X. G. Zhang, B. X. Han, *Clean Soil Air Water* **2007**, *35*, 223–229.
[16] a) D. Shen, R. Zhang, B. X. Han, Y. Dong, W. Wu, J. L. Zhang, J. C. Li, T. Jiang, Z. M. Liu, *Chem. Eur. J.* **2004**, *10*, 5123–5128; b) D. Shen, B. X. Han, Y. Dong, W. Wu, J. Chen, J. L. Zhang, *Chem. Eur. J.* **2005**, *11*, 1228–1234.
[17] W. Li, J. L. Zhang, B. X. Han, S. Q. Cheng, C. X. Zhang, X. Y. Feng, *Langmuir* **2009**, *25*, 196–202.
[18] J. L. Zhang, B. X. Han, C. X. Zhang, W. Li, X. Y. Feng, *Angew. Chem.* **2008**, *120*, 3054–3057; *Angew. Chem. Int. Ed.* **2008**, *47*, 3012–3015.
[19] J. L. Zhang, B. X. Han, W. Li, Y. J. Zhao, M. Q. Hou, *Angew. Chem.* **2008**, *120*, 10273–10277; *Angew. Chem. Int. Ed.* **2008**, *47*, 10119–10123.
[20] K. P. Johnston, K. L. Harrison, M. J. Clarke, S. M. Howdle, M. P. Heitz, F. V. Bright, C. Carlier, T. W. Randolph, *Science* **1996**, *271*, 624–626.
[21] P. G. Jessop, B. Subramaniam, *Chem. Rev.* **2007**, *107*, 2666–2694.
[22] K. L. Herrington, E. W. Kaler, D. D. Miller, J. A. Zasadzinski, S. Chiruvolu, *J. Phys. Chem.* **1993**, *97*, 13792–13802.
[23] H. Q. Yin, J. B. Huang, Y. Y. Lin, Y. Y. Zhang, S. C. Qiu, J. P. Ye, *J. Phys. Chem. B* **2005**, *109*, 4104–4110.
[24] a) P. Bhargava, Y. F. Tu, J. X. Zheng, H. M. Xiong, R. P. Quirk, *J. Am. Chem. Soc.* **2007**, *129*, 1113–1121; b) M. Rosa, M. R. Infante, M. D. G. Miguel, B. Lindman, *Langmuir* **2006**, *22*, 5588–5596.
[25] O. Söderman, K. L. Herrington, E. W. Kaler, D. D. Miller, *Langmuir* **1997**, *13*, 5531–5538.
[26] D. D. Miller, D. F. Evans, *J. Phys. Chem.* **1989**, *93*, 323–333.
[27] a) M. Almgren, J. E. J. Löroth, *J. Colloid Interface Sci.* **1981**, *81*, 486–489; b) M. Almgren, *Adv. Colloid Interface Sci.* **1992**, *41*, 9–18; c) M. H. Gehlen, F. C. De Schryver, *Chem. Rev.* **1993**, *93*, 199–221.
[28] a) F. Caruso, F. Grieser, A. Murphy, P. Thistlethwaite, R. Urquhart, M. Almgren, E. Wistus, *J. Am. Chem. Soc.* **1991**, *113*, 4838–4843; b) B. Medhage, M. Almgren, *J. Fluoresc.* **1992**, *2*, 7–10.
[29] a) A. Pizzino, M. P. Rodriguez, C. Xuereb, M. Catté, E. V. Hecke, J. M. Aubry, J. L. Salager, *Langmuir* **2007**, *23*, 5286–5291; b) J. Allouche, E. Tyrode, V. Sadtler, L. Choplin, J. L. Salager, *Langmuir* **2004**, *20*, 2134–2138.
[30] a) L. M. Zhai, J. Y. Zhang, Q. X. Shi, W. J. Chen, M. Zhao, *J. Colloid Interface Sci.* **2005**, *284*, 698–703; b) A. Mohanty, T. Patra, J. Dey, *J. Phys. Chem. B* **2007**, *111*, 7155–7159.
[31] D. X. Liu, J. L. Zhang, B. X. Han, J. F. Fan, T. C. Mu, Z. M. Liu, W. Z. Wu, J. Chen, *J. Chem. Phys.* **2003**, *119*, 4873–4878.
[32] A. Bernheim-Groswasser, R. Zana, Y. Talmon, *J. Phys. Chem. B* **2000**, *104*, 12192–12201.
[33] a) T. Asakawa, S. Miyagishi, *Langmuir* **1999**, *15*, 3464–3467; b) T. Asakawa, S. Ishino, P. Hansson, M. Almgren, A. Ohta, S. Miyagishi, *Langmuir* **2004**, *20*, 6998–7001; c) S. Miyagishi, T. Asakawa, A. Ohta, *Mixed Surfactant Systems*, 2nd. ed., Marcel Dekker, New York, **2005**, pp. 431–432.
[34] a) I. Krishnamoorthy, G. Krishnamoorthy, *J. Phys. Chem. B* **2001**, *15*, 1484–1486; b) P. J. G. Coutinho, E. M. S. Castanheira, M. C. Rei, M. E. Oliveira, *J. Phys. Chem. B* **2002**, *106*, 12841–12844; c) G. Hungerford, E. M. S. Castanheira, A. L. F. Baptista, P. J. G. Coutinho, M. E. Oliveira, *J. Fluoresc.* **2005**, *15*, 835–838.
[35] A. Cser, K. Nagy, L. Biczók, *Chem. Phys. Lett.* **2002**, *360*, 473–475.
[36] a) M. C. A. Stuart, J. C. Pas, J. B. Engberts, *J. Phys. Org. Chem.* **2005**, *18*, 929–934; b) L. Wasungu, M. C. A. Stuart, M. Scarzello, J. B. Engberts, D. Hoekstra, *J. Biochim. Biophys. Acta* **2006**, *1758*, 1677–1684.
[37] F. R. Alves, M. E. D. Zaniquelli, W. Loh, E. M. S. Castanheira, M. Elisabete, R. Oliveira, E. Feitosa, *J. Colloid Interface Sci.* **2007**, *316*, 132–139.
[38] M. C. A. Stuart, E. Boekema, *J. Biochim. Biophys. Acta* **2007**, *1768*, 2681–2689.
[39] K. Kalyanasundaram, J. K. Thomas, *J. Am. Chem. Soc.* **1977**, *99*, 2039–2041.
[40] T. Kodama, A. Ohta, K. Toda, T. Katada, T. Asakawa, S. Miyagishi, *Colloids Surf. A* **2006**, *277*, 20–26.
[41] J. Ulmius, B. Lindman, G. Lindblom, T. Drakenberg, *J. Colloid Interface Sci.* **1978**, *65*, 88–90.
[42] S. Miyagishi, H. Kurimoto, Y. Ishihara, T. Asakawa, *Bull. Chem. Soc. Jpn.* **1994**, *67*, 2398–2399.
[43] J. M. O'Callaghan, M. P. Copley, J. P. Hanrahan, M. A. Morris, D. C. Steytler, R. K. Heenan, R. Staudt, J. D. Holmes, *Langmuir* **2008**, *24*, 6959–6964.
[44] a) E. Feitosa, N. M. Bonassi, W. Loh, *Langmuir* **2006**, *22*, 4512–4517; b) P. C. A. Barreleiro, G. Olofsson, W. Brown, K. Edwards, N. M. Bonassi, E. Feitosa, *Langmuir* **2002**, *18*, 1024–1029.
[45] M. T. Allen, L. Miola, D. G. Whitten, *J. Am. Chem. Soc.* **1988**, *110*, 3198–3206.
[46] a) X. J. Zhang, D. Li, *Angew. Chem.* **2006**, *118*, 6117–6120; *Angew. Chem. Int. Ed.* **2006**, *45*, 5971–5974; b) B. Tan, H. J. Lehmler, S. M. Vyas, B. L. Knutson, S. E. Rankin, *Adv. Mater.* **2005**, *17*, 2368–2371.
[47] A. Fidalgo, L. M. Ilharco, *Chem. Eur. J.* **2004**, *10*, 392–398.
[48] H. L. Clever, *Solubility Data Series, Vol. 1: Helium and Nenon*, Pergamon Press, Oxford, **1981**, pp. 128–129.
[49] R. G. Zielinski, E. W. Kaler, M. E. Paulaitis, *J. Phys. Chem.* **1995**, *99*, 10354–10358.
[50] G. D. Bothun, B. L. Knutson, H. J. Strobel, S. E. Nokes, *Langmuir* **2005**, *21*, 530–536.
[51] a) J. N. Israelachvili, D. J. Mitchell, B. W. Ninham, *J. Chem. Soc. Faraday Trans. 2* **1976**, *72*, 1525–1527; b) J. N. Israelachvili, D. J. Mitchell, B. W. Ninham, *Biochim. Biophys. Acta Biomembr.* **1977**, *470*, 185–187; c) J. N. Israelachvili, S. Marcelja, R. G. Q. Horn, *Q. Rev. Biophys.* **1980**, *13*, 121–123.

[52] H. L. Clever, D. M. Mason, C. L. Young, *Solubility Data Series, Carbon Dioxide*, Pergamon Press, Oxford, **1992**, pp, 241–242.
[53] a) N. Vlachy, M. Drechsler, J. M. Verbavatz, D. Touraud, W. Kunz, *J. Colloid Interface Sci.* **2008**, *319*, 542–548; b) Y. W. Shen, J. C. Hao, H. Hoffmann, *Soft Matter* **2007**, *3*, 1407–1412.
[54] D. Li, B. X. Han, *Macromolecules* **2000**, *33*, 4555–4558.
[55] R. Zhang, J. Liu, J. He, B. X. Han, *Macromolecules* **2002**, *35*, 7869–7871.
[56] D. Shen, B. X. Han, Y. Dong, J. Chen, T. C. Mu, W. Z. Wu, J. L. Zhang, *J. Phys. Chem. B* **2005**, *109*, 5796–5799.
[57] D. X. Liu, J. L. Zhang, J. F. Fan, B. X. Han, J. Chen, *J. Phys. Chem. B* **2004**, *108*, 2851–2856.
[58] O. Sondeman, K. L. Herrington, E. W. Kaler, D. D. Miller, *Langmuir* **1997**, *13*, 5531–5534.
[59] a) M. T. Allen, L. Miola, D. G. Whitten, *J. Am. Chem. Soc.* **1988**, *110*, 3198–3200; b) M. T. Allen, L. Miola, D. M. Shin, B. R. Sudaby, D. G. Whitten, *J. Membr. Sci.* **1987**, *33*, 201–203.
[60] P. C. A. Barreleiro, G. Olofsson, N. M. Bonasssi, E. Feitosa, *Langmuir* **2002**, *18*, 1024–1025.

Received: September 7, 2009
Published online: December 8, 2009

